A New Radiotherapy Optimization Model Based on Equivalent Uniform Dose

CAIPING GUO[iD]

Electronic Engineering Department, Taiyuan Institute of Technology, Taiyuan 030008, China

e-mail: guocaipingvip@163.com

ABSTRACT Optimization model based on generalized equivalent uniform dose (gEUD) linear sub-score or quadratic sub-score, which only penalizes doses higher or lower than the prescribed dose $gEUD_0$, has the shortcomings of semi-deviation, vanishing gradient and non-increasing in the feasible solution space. When gradient-based optimization algorithms are used to solve the radiotherapy inverse optimization problem, these algorithms may get trapped in a local minimum. To address these drawbacks, this study proposes a new gEUD-based optimization model based on regularization theory. In the new optimization model, a dosage whether lower or higher than the prescribed dose is assigned different penalties. To test its efficiency, it was tested on a phantom TG119, and two types of clinic cases(one prostate cancer case and one head and neck cancer case). The improved optimization model was compared with unimproved gEUD-based optimization model. Additionally, the improved gEUD-based optimization model was compared with another improved gEUD-based linear optimization model proposed by us. The gradient-based optimization algorithm(L-BFGS) was applied to solve these large-scale optimization problems. Optimization based on our improved optimization model is capable of improving the organs at risk (OARS) sparing while maintaining the same planning target volume (PTV) coverage. In practice, although the DV-based optimization should be able to gain a similar plan, parameters adjustment of the optimization model is time-consuming. The new gEUD-based hybrid physical–biological optimization model has the potential to expand the solution space and improve the quality of radiotherapy plan.

INDEX TERMS Intensity-modulated radiation therapy, gEUD, hybrid criteria, regularization.

I. INTRODUCTION

Intensity Modulated Radiation Therapy (IMRT) is currently one of the effective methods for the treatment of malignant tumors. To ensure that the tumor control probability (TCP) reaches a certain level of treatment, the normal tissue complications probability (NTCP) is below a certain level, and the lowest possible dose is obtained for the organs at risk, IMRT can be used to adjust the irradiation angle, ray intensity, and dose distribution on the tumor area [1].

The key technology and main task of IMRT is to devise an acceptable plan through the inverse problem. The pro-

The associate editor coordinating the review of this manuscript and approving it for publication was Yizhang Jiang[iD].

cess of the solution is defined as inverse planning, the key link of which is to solve intensity distributions of external beams that determine the quality of radiotherapy. Furthermore, in inverse planning, the quality of an optimized treatment plan is affected by the optimization model and the optimization algorithm [2].

The optimization model is an important indicator for evaluating and optimizing treatment plans. It is not only a tool for evaluating treatment plans, but also a link connecting input radiation parameters and output dose distributions. It also has an impact on the optimization algorithm's ability [2]. Optimization models applied in radiotherapy planning mainly include organ-based model, voxel-based model and dose volume histogram (DVH)-based model [3]. These optimization

models were often defined as the weighted sum of sub-scores for all organs under the optimization [2], [4]–[7]. Compared with physical criteria in the optimization based on organ-based model, biological criteria can comprehensively consider tissue performance and its potential nonlinear radiation effects, and have the potential to predict the biological effects of tumors and normal tissues [8]. Therefore, the study of objective functions based on biological criteria has attracted people's attention [2], [9]–[19]. Biological criteria include TCP, NTCP and gEUD (generalized equivalent uniform dose). Because of the uncertainty associated with TCP and NTCP, they have not been widely applied in radiotherapy inverse planning systems. gEUD-based optimization's advantages, however, has been investigated by several scholars, and the Varian radiotherapy planning system also has a built-in optimization method based on gEUD [12]. By comparing with the gEUD-based biological optimization method, the experiments of Hartmann and Bogner [13] and Dirscherl *et al.* [14] verified the advantages of the gEUD-based hybrid criteria optimization models. In these optimization models, the gEUD-based sub-scores were transformed into linear and quadratic objective functions. A gEUD-based sub-score that penalizes the square of the absolute difference between the actual dose and the prescribed dose was proposed by Dirscherl *et al.* For gEUD that do not satisfy the set value during the optimization process, Widescott *et al.* [15] and Schwarz *et al.* [16] proposed a sub-score of the relative deviation square for gEUD, Wu *et al.* [17], Mihailidis *et al.* [18] and Lee *et al.* [19] used a gEUD-based linear sub-score penalizing relative deviation between the actual and the prescribed $gEUD_0$.

Gradient-based optimization algorithms are widely used to solve the radiotherapy inverse optimization problems in commercial inverse planning systems(HELIOS and Pinnacle) because of their speed [11]. The major concern when using those algorithms is that the optimization iterations may get trapped in a local minimum. Nevertheless, when the relative deviation-based optimization models mentioned above are solved by gradient algorithms, the problems of semi-deviation and the vanishing gradient are introduced. These problems will lead to the loss of better solutions in the feasible solution space. To expand the ability of the optimization models to search the solution space, several researchers have done much work. Zarepisheh *et al.* [3] proposed that when the optimization model was increasing function, the Pareto optimality was guaranteed. To avoid discontinuous gradients, which may restrain gradient-based optimization algorithms, the positive part operators that constitute the DVH optimization models are regularized by Fredriksson [20]. Zhang *et al.* [21] verified that the problem of vanishing gradient led to the poor convergence properties of conventional optimization models. Mai *et al.* [7] proposed and evaluated a voxel-based quadratic model optimization model. Guo *et al.* [2] proposed new quadratic sub-scores for the maximum dose criterion and the gEUD criterion to

overcome the drawbacks of semi-deviation and the vanishing gradient.

Next, we take the gEUD-based sub-score shown in (1) for example to illustrate the shortcomings of this kind of sub-score. gEUD is the actual dose, and $gEUD_0$ is the prescribed dose. $H(\cdot)$ is the step function. Then

$$
\begin{aligned}
f(gEUD(\boldsymbol{D}) - gEUD_0) &= H(gEUD(\boldsymbol{D}), gEUD_0) \\
&\times (gEUD(\boldsymbol{D}) - gEUD_0) \\
&= max(gEUD(\boldsymbol{D}) - gEUD_0, 0) \quad (1)
\end{aligned}
$$

(1) Semi-deviation penalties. The organ constrained by the sub-score (1) is assigned a linear penalty if and only if $gEUD \geq gEUD_0$; otherwise, the penalty is zero. In this case, reducing the dose to prescribed $gEUD_0$ is the only incentive of optimization, even though a better solution with a lower gEUD can be gained without there is no reduction other treatment goals.

(2) Vanishing gradient in the feasible solution space. If the actual gEUD in (1) is less than or equal to $gEUD_0$, the max function equals to zero, so gradients in the interior of the feasible solution space is equal to zero. If there is a feasible point in the solution space, gradient based optimization algorithm predicts difficultly the step length.

(3) Non-increasing function. The sub-score (1) in is not an increasing function, because it does not differentiate the doses that are lower than the reference dose $gEUD_0$. Hence, Pareto optimality might be lost [3].

Because of the above problems, the search capability of the gradient-based optimization algorithm is limited. The improvement to the quadratic model has been reported [2]. In this study, we proposed and assessed a new gEUD-based hybrid physical-biological optimization model based on regularization theory without the three problems described above. To test its efficiency, the new gEUD-based optimization model was tested on three types of cases.

In the following sections, we describe in detail the materials and methods contained in the proposed method in Section II. Then experimental results are presented in Section III, and finally discuss the results and future direction of research in Section IV and V.

II. MATERIALS AND METHODS
A. OVERALL RESEARCH FLOW
In this study. we proposed and assessed a novel gEUD-based optimization model. The new optimization model was used to solve the inverse problem of fluence map optimization (FMO). A gradient-based optimization algorithm (L-BFGS) was used to solve the large-scale, constrained optimization problem [2], [4]–[7], [11]. The square roots of the beamlet weights were used as optimized variables to avoid non-physical solutions [2], [4]–[6], [11]. The overall research flow is shown in Fig.1. First a new gEUD-based optimization model was proposed based on regularization theory, then it was tested on three kinds of cases after setting treatment
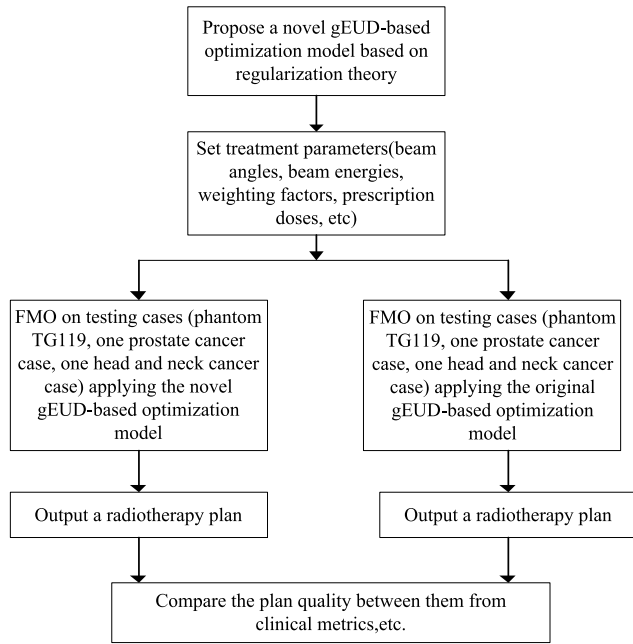
FIGURE 1. Overall research flow.

parameters, and last the quality of the improved plan optimized by applying the new optimization model was evaluated by comparing with the unimproved plan optimized by applying the original optimization model from clinical metrics.

B. REGULARIZATION THEORY AND A NOVEL OPTIMIZATION MODEL

1) REGULARIZATION OF MAX FUNCTION

To solve the shortcomings of the *max* functions described above in Section I, convex regularization can be used to transfer the max functions into smooth functions with everywhere nonzero gradients [22]. A common smooth and convex regularization of *max* functions is the *log-sum-exp* function, which is defined as

$$lse_\varepsilon(x_1, \cdots, x_n) = \varepsilon \ln(\sum_{i=1}^{n} \exp(x_i/\varepsilon)) \quad (2)$$

where $\varepsilon > 0$ is a parameter determined the exactness of the regularization. As $\varepsilon \to 0$, the regularized function converges uniformly to the corresponding max function, which is given by

$$\lim_{\varepsilon \to 0} \varepsilon \ln(\sum_{i=1}^{n} \exp(x_i/\varepsilon)) = max(x_1, \cdots, x_n) \quad (3)$$

In linear gEUD-based sub-score described in (1), it is the case that $n = 2$ with one of the arguments being 0; the regularized *max* function is given by

$$max(x, 0) \approx lse_\varepsilon(x, 0) = \varepsilon ln(exp(\frac{x}{\varepsilon}) + 1) \quad (4)$$

The comparison results between the *max* function and the regularized function($\varepsilon = 1$ and $\varepsilon = 0.01$) are illustrated in Fig.2. Fig.2.b is the detail part of Fig.2.a. We can see from
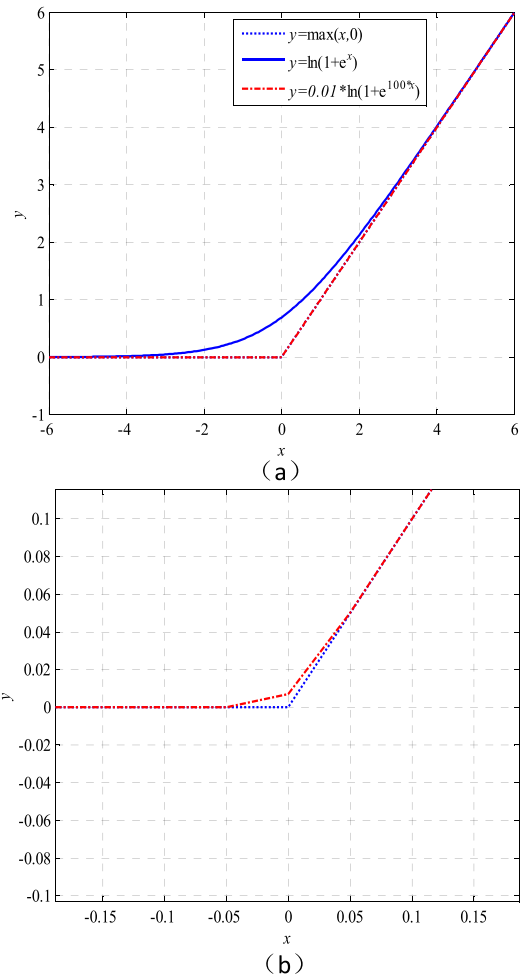

FIGURE 2. An illustration of regularized function ($\varepsilon = 1$ and $\varepsilon = 0.01$) and $max(x, 0)$. (b) is the detail part in (a).

the Fig.2: (1) As $\varepsilon = 0.01$, the regularized function is close to the original max function, and $\varepsilon \to 0$, the regularized function converges uniformly to the corresponding max; (2) The regularized function gives all the actual dose that is higher or lower than the prescribed dose different degrees punishment, and it is an increasing function with continuous gradients everywhere.

2) A NOVEL gEUD-BASED HYBRID CRITERIA OPTIMIZATION MODEL

Hartmann and Bogner [13] and Dirscherl *et al.* [14] have shown that treatment plans based on gEUD hybrid criteria optimization models are superior to those based on gEUD-based biological models alone. According to these findings, the original gEUD-based optimization model used in our study can be expressed as

$$\min_{x \geq 0} \sum_{\sigma \in C} \omega^\sigma \max(gEUD(\boldsymbol{D}) - gEUD_{\sigma 0}, 0)$$

$$+ \sum_{\vartheta \in T} \omega^\vartheta \frac{1}{N_\vartheta} \sum_{j \in v_\vartheta} (\omega_j x - D_{mean}^\vartheta)^2 \quad (5)$$

In the above, $gEUD$ and $gEUD_0$ represent the actual dose and the prescribed dose, respectively. C and T represent the collection of OARs and PTV, respectively, and υ_ϑ denotes the set of voxels in PTV ϑ. The number of voxels in PTV are represented by N_ϑ. ω^σ and ω^ϑ are the weighting factors, representing the clinical significance of corresponding sub-objective function and determined by trial and error. $gEUD_{\sigma 0}$ and D^ϑ_{mean} stand for the prescribed $gEUD$ dose to OAR σ and prescribed mean dose to target ϑ, respectively. ω_j computed using CERR's pencil beam algorithm (QIB), is the jth row of dose deposition matrix W, and x is the optimized vector of beamlet weights (i.e., fluence elements).

According to (4), the regularized $gEUD$ sub-score can be defined as

$$max(x, 0)|_{x=gEUD(D)-gEUD_{\sigma 0}}$$
$$\approx lse_\varepsilon(gEUD(D) - gEUD_{\sigma 0}, 0)$$
$$= \varepsilon ln(exp(\frac{gEUD(D) - gEUD_{\sigma 0}}{\varepsilon}) + 1) \quad (6)$$

In the above regularized $gEUD$ sub-score, the problems of semi-deviation, vanishing gradient and non-increasing are solved. The new gEUD-based optimization model is given by

$$\min_{x \geq 0} \sum_{\sigma \in C} \omega^\sigma \varepsilon \ln(\exp(\frac{gEUD(D) - gEUD_{\sigma 0}}{\varepsilon}) + 1)$$
$$+ \sum_{\vartheta \in T} \omega^\vartheta \frac{1}{N_\vartheta} \sum_{j \in v_\vartheta} (D_j - D^\vartheta_{mean})^2 \quad (7)$$

In (7), ε is regularization parameter. In order to simplify the optimization process, a fixed value is adopted in this paper, let $\varepsilon = 1$. For OAR σ, whether the actual dose gEUD is less than or higher than $gEUD_{\sigma 0}$, the organ constrained by the regularized gEUD sub-score is given varying degrees of punishment. $gEUD(D)$ is defined as [23]

$$gEUD(D) = \left(\frac{1}{N} \sum_{j=1}^{N} D_j^a\right)^{1/a} \quad (8)$$

N is the number of voxels in the optimized structure, a is the tissue-specific parameter reflcting the dose-volume effect, and $D_j = w_j x$ is the dose to voxel j. For normal tissue and OAR, a is defined as more than one, and function (8) is a convex function [24]; otherwise it is a concave function.

The gradient-based optimization algorithm (L-BFGS) need the first derivatives of sub-scores in optimization model to update the inverse Hessian matrix and determine the step length. The first derivatives of all sub-scores contained in (5) and (7) can be illustrated as follows:

- Original gEUD sub-score in (1)

$$\frac{\partial f_{gEUD}}{\partial x_j} = max(gEUD(D) - gEUD_0, 0)$$
$$\cdot \frac{gEUD(D)}{gEUD_0 \sum_{i=1}^{N} D_i^a} \sum_{i=1}^{N} D_i^{a-1} W_{i,j} \quad (9)$$

Here, $D_i = \omega_i x$, $W_{i,j}$ is the (i, j)th element of the dose deposition matrix W.
- Regularized gEUD sub-score in (6)

$$\frac{\partial f_{gEUD}}{\partial x_j} = \frac{\varepsilon \cdot exp(\frac{gEUD(D)-gEUD_0}{\varepsilon})}{exp(\frac{gEUD(D)-gEUD_0}{\varepsilon}) + 1}$$
$$\cdot \frac{gEUD(D)}{\varepsilon \sum_{i=1}^{N} D_i^a} \sum_{i=1}^{N} D_i^{a-1} W_{i,j} \quad (10)$$

- Mean dose sub-score

$$\frac{\partial f_{mean}}{\partial x_j} = \frac{2}{N} \sum_{i=1}^{N} (D_i - D_{mean}) W_{i,j} \quad (11)$$

C. TEST CASES
1) TG119 DATASET
Testing phantom TG119 [25] includes a C-shaped target (OuterTarget) and an OAR (Core) wrapped around by target. The prescribed $gEUD_0$ for Core was 0.4 Gy, and prescribed D_{mean} for OuterTarget was 1 Gy. Additionally, a = 3 was used for gEUD. Five coplanar 6MV photon beams spaced equally were used for planning.

2) CLINICAL CASE
The feasibility and performance of the novel optimization model was tested on one prostate cancer case and one head and neck (HN) cancer case randomly selected from the database of treated cases. The study protocols were approved by the Ethics Committee of the North University of China with the approval No. 2018006, the written consent forms were signed by the participants whose computed tomography (CT) images were used for this study.

For one prostate cancer case, two OARs (Rectum and Bladder) and a PTV were contained in the optimization model. The prescribed mean dose to PTV is 80Gy. It required at least 99% of the PTV volume to receive 95% of the prescribed mean dose. Table 1 lists the radiobiological parameters and prescribed dose of gEUD sub-score derived from the literature [26], [27]. Five coplanar beams of 6-MV photons were applied for planning, with the gantry placed at 36°, 100°, 180°, 260°, and 324°.

For head and neck cancer (HN) case, three PTVs (PTV56Gy, PTV63Gy, and PTV70Gy) and four OARs (L-Parotid, R-Parotid, Spinal cord, and Brainstem) were considered into the optimization model. These PTVs were considered simultaneously with 56 Gy, 63 Gy, and 70Gy, respectively. As shown in Table 1, the prescribed $gEUD_0$ for brainstem and spinal cord were 40 Gy and 30 Gy, respectively [17], and for Bilateral Parotids was 35 Gy [28]. Seven equally spaced coplanar 6-MV photons beams were used for planning.

D. EXPERIMENTAL ENVIRONMENT AND ASSESSMENT CRITERIA

Computational Environment for Radiotherapy Research (i.e., CERR) version 4.0 [29] was used as our radiotherapy planning platform. All experiments were performed by using an instrument equipped with a 32-bit OS, Windows 7, and an Intel (R) Core (TM) i3-4150 CPU with 4G RAM.

The clinical evaluation guidelines shown in Table 2 [30] and the dose constraints of OARs [26], [27] in Table 3 were used to assed the plan quality. In order to obtain a better target dose characteristic for HN cancer, we relax the average dose of parotid gland to 30Gy, because patients whose average dose of parotid gland is between 26-30Gy can gradually recover the function of parotid gland 12 months after radiotherapy [31]. Conformity index (CI) and homogeneity index (HI) [26] are, respectively, used to evaluate the conformity and homogeneity of the PTV.

A Wilcoxon matched pairs signed ranks test using a significant level of 5% was used to analyze the significant difference between the unimproved plan and the improved plan.

III. RESULTS

A. PLANS COMPARISON TSETING ON TG119

Fig.3 shows the comparison results on the TG119 testing phantom between the improved plan optimized applying gEUD-based hybrid criteria optimization model (7) and the unimproved plan using original gEUD-based hybrid criteria optimization model (5). In these optimization model, the combination of weighting factors for Outer Target and Core is (2,0.1). The solid line represents the improved plan denoted by 0.1, and the dotted line represents the unimproved plan denoted by Unimproved. We see that the improved plan outperformed the Unimproved plan in terms of Core sparing while maintaining similar dose coverage of Outer Target. To test the influence of the combination of different weighting factors on the optimization results, we keep the weighting factors of the Outer Target unchanged in improved model, and then decrease and increase the weighting factor of core to 0.05 and 0.15 respectively. The optimization results, marked with 0.05 and 0.15 respectively, are shown in Fig.4. It can be seen that the greater the weighting factors for the Core sub-score, the smaller the dose within the Core, whereas the dose coverage within the Outer Target increased because of the trade-off, and vice versa.

B. PLAN COMPARISONS TSETING ON CLINICAL CASES

We performed gEUD-based hybrid criteria optimization with improved and unimproved optimization models on clinical cases. The weighting factors of sub-scores contained in improved and unimproved optimization models are listed in Table 4. Fig.4 and Fig.5 show the DVH comparisons between the plans with unimproved optimization model in (5) and improved optimization model in (7) for prostate cancer case and HN cancer case, respectively. To make clear and detail comparisons, Table 5 and Table 6 show some clinical metrics
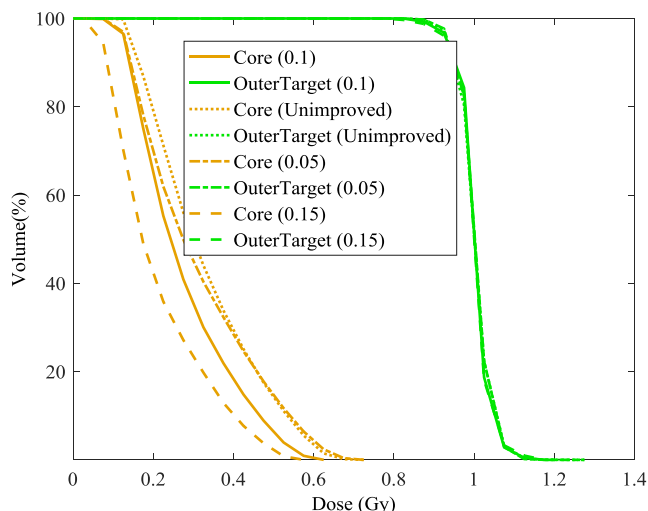

FIGURE 3. DVH comparison between the improved plan and the unimproved plan on TG119.
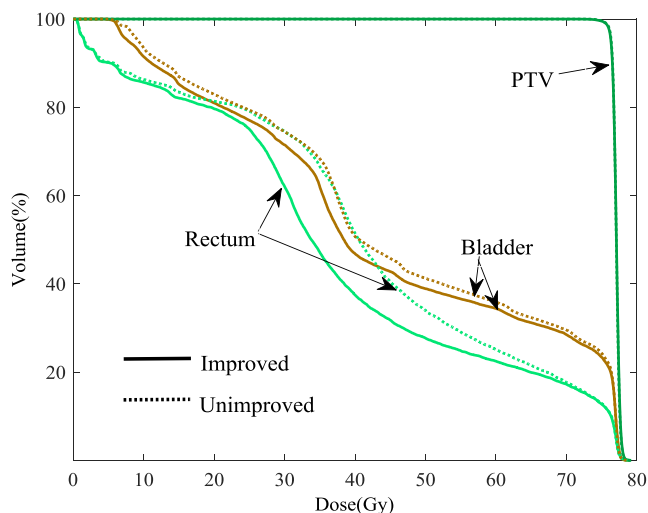

FIGURE 4. DVH comparison between the improved plan and the unimproved plan on prostate cancer case.

for two types of clinical cases corresponding to the DVH endpoint values in Fig.4 and Fig.5.

Experimental results above showed that the quality of the improved plan optimized based on the new optimization model outperformed that of the unimproved plan considering OARs protection while maintaining a similar dose to PTV(s). The DVHs of the PTV(s) were very similar in terms of coverage and homogeneity. The most significant differences were observed while investigating the DVH curves for the OARs rectum, cord and brainstem. In improved prostate plan shown in Fig.4 and Table 5, compared with the plan optimized based on the original optimization model, the clinically relevant DV constraints in Table2 rectal V_{50Gy}, V_{60Gy}, V_{65Gy}, V_{70Gy} and V_{75Gy} as well as D_{mean} were respectively reduced by 18.39%, 10.58%, 7.74%, 2.38%, 1.70% and 9.41%, bladder V_{65Gy}, V_{70Gy} and V_{75Gy} were respectively reduced by 3.56%, 3.62%

TABLE 1. gEUD-based optimization parameters for prostate cancer and head and neck cancer.

Cases	Prostate		Head and neck			
Organs	Rectum	Bladder	Cord	Brainstem	L-Parotid	R-Parotid
gEUD$_0$(Gy)	35	35	35	40	20	20
a	8	8	7.4	4.6	5	5

TABLE 2. Clinical evaluation guidelines for bladder and rectum.

OAR			Parameters of DV constraints			
Bladder			$V_{65}<50\%$	$V_{70}<35\%$	$V_{75}<25\%$	$V_{80}<15\%$
Rectum	$V_{50}<50\%$	$V_{60}<35\%$	$V_{65}<25\%$	$V_{70}<20\%$	$V_{75}<15\%$	
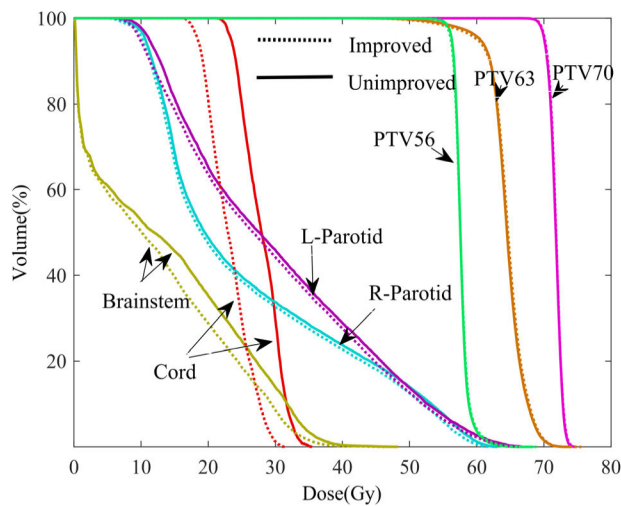
FIGURE 5. DVH comparison between the improved plan and the unimproved plan on HN cancer case.

TABLE 3. Dose constraints of OARs.

Case	Organs	Constraints
Prostate	Rectum	$D_{max}<80Gy$
	Bladder	$D_{max}<80Gy$
Head and neck	Cord	$D_{max}<45Gy$
	Brainstem	$D_{max}<50Gy$
	L-Parotid	$D_{mean}<30Gy$
	R-Parotid	$D_{mean}<30Gy$
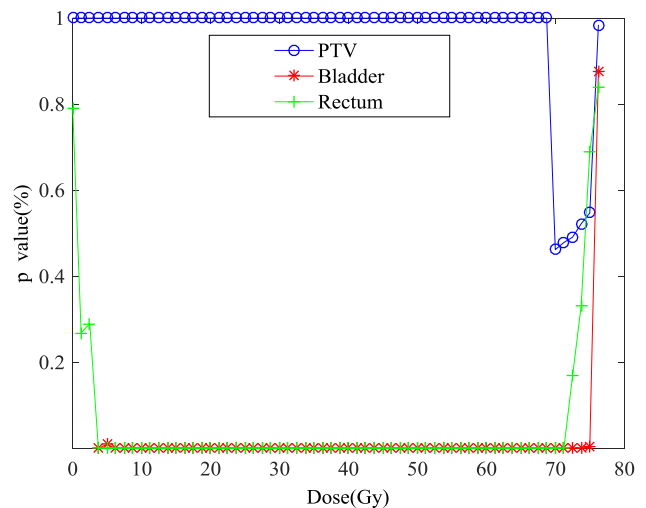
FIGURE 6. p values for the different dose bins of DVH from Figure 4.

and 3.95%. In improved HN plan shown in Fig.5 and Table 6, D_{max} and D_{mean} to cord decreased, respectively, by 3.31 and 10.93%, and D_{max} and D_{mean} to brainstem decreased by 11.41% and 17.16%, respectively. The parallel organs L-Parotid V_{30Gy}, V_{50Gy} and D_{mean} were recorded decrease of 3.53%,8.43% and 2.94%; the R-Parotid V_{30Gy}, V_{50Gy} and D_{mean} were also recorded decrease of 3.29%,10.86% and 2.63%, respectively. The decrease of the D_{max} to the serial organs spinal cord and brainstem is beneficial to the reduction of their complications. Meanwhile, the reduction of the D_{mean}, V_{30Gy} and $_{50Gy}$ to the parotid glands contributes to the reduction of their complications.

We calculated p values (Wilcoxon test) for the different dose bins of DVH from Fig.4 and Fig.5. Significant differences were observed between the improved plan and unimproved plan for the Bladder and Rectum (Fig.4) at between 4 Gy to72Gy ($p<0.05$), as illustrated in figure 6. For the Cord (Fig.6)), significant differences were observed in dose higher than 15Gy, and for the Brainstem, significant differences were observed in the dose higher than 4Gy. For the L-Parotid

and R-Parotid, significant differences were observed in the dose higher than 5Gy. PTV coverage, for different cases and different optimization methods, was maintained.

C. INFLUENCE OF REGULARIZATION PARAMETER

The influence of regularization parameters ε on optimization results was investigated. The prostate cancer case as an example was used to analyze the influence of regularization

TABLE 4. Weighting factors of sub-scores for clinical cases.

Case	Organs	Unimproved	Improved
prostate	PTV	93	91
	Rectun	2	3
	Bladder	5	6
Head and neck	PTV70Gy	15	14
	PTV63Gy	9	7
	PTV56Gy	14	9
	Cord	2	2
	Brainstem	1	1
	L-Parotid	8	8
	R-Parotid	20	20

TABLE 5. Clinical metrics in Fig.4 for prostate cancer.

Organ	Clinical metrics	Unimproved	Improved
PTV	$D_{5\%}$(Gy)	77.77	77.80
	$D_{95\%}$(Gy)	76.37	76.36
	D_{mean}(Gy)	77.10	77.10
	HI	1.02	1.02
	CI	0.88	0.90
Rectum	V_{50Gy}(%)	33.93	27.69
	V_{60Gy}(%)	25.13	22.47
	V_{65Gy}(%)	21.58	19.91
	V_{70Gy}(%)	17.67	17.25
	V_{75Gy}(%)	12.95	12.73
	D_{mean}(Gy)	42.10	38.14
Bladder	V_{65Gy}(%)	32.34	31.19
	V_{70Gy}(%)	29.55	28.48
	V_{75Gy}(%)	24.33	23.37
	D_{mean}(Gy)	46.60	44.89

parameters on the quality of plan. The comparative results of the treatment plans based on the unimproved and improved gEUD-based optimization models ($\varepsilon = 1$ and $\varepsilon = 0.1$) are shown in Fig.7 (a), Fig.7(b) shows the details of the Fig.7(a). Fig.7(c) shows the comparison results of plans optimized with the improved gEUD-based optimization model ($\varepsilon = 0.5, \varepsilon = 1$ and $\varepsilon = 1.5$). Fig.7(d) is the detail part of the Fig.7(c). From Fig.7(a)-(b), we can conclude that the improved plan quality with $\varepsilon = 0.1$ is similar to that of the unimproved plan, which is accordance with the equation (3). With the increase of ε, the difference between the new gEUD sub-score proposed based on the regularization theory and the original linear gEUD sub-score in the form of the max function increases, the difference between the optimization results optimized based on them also increases, and the more obvious the advantages of the improved optimization model

are. In the improved plan quality with $\varepsilon = 1$, the DVH curves and clinical metrics for the rectum and bladder were significantly improved while maintaining a similar dose to the PTV. Compared with the improved plan with $\varepsilon = 1$, the quality of the improved plan with $\varepsilon = 0.5$ is better when considering the dose to OARs. However, the dose coverage of PTV decreased because of the trade-off. The quality of the improved plans with $\varepsilon = 1.5$ and $\varepsilon = 1$ is similar in terms of OARs sparing and PTV coverage.

IV. DISCUSSIONS

Experimental results show that the quality of the improved plan outperformed that of the unimproved plan considering OARs protection while maintaining a similar dose to the PTV(s). These improvements observed owing to the new gEUD sub-score can be attributed to the following

TABLE 6. Clinical metrics in Fig. 5 for HN cancer.

Organ	Clinical metrics	Unimproved	Improved
PTV70Gy	$D_{5\%}(Gy)$	73.09	73.16
	$D_{95\%}(Gy)$	70.07	70.17
	$D_{mean}(Gy)$	71.74	71.79
	HI	1.04	1.04
	CI	0.83	0.84
PTV63Gy	$D_{5\%}(Gy)$	68.65	68.78
	$D_{95\%}(Gy)$	60.55	60.53
	$D_{mean}(Gy)$	65.51	64.58
	HI	1.13	1.13
	CI	0.67	0.67
PTV56Gy	$D_{5\%}(Gy)$	59.60	59.70
	$D_{95\%}(Gy)$	56.19	56.15
	$D_{mean}(Gy)$	57.71	57.70
	HI	1.06	1.06
	CI	0.56	0.57
Brainstem	$D_{max}(Gy)$	48.28	46.68
	$D_{mean}(Gy)$	13.82	12.31
Cord	$D_{max}(Gy)$	35.48	31.43
	$D_{mean}(Gy)$	27.97	23.17
L-Parotid	$V_{30Gy}(\%)$	45.89	44.27
	$V_{50Gy}(\%)$	13.76	12.60
	$D_{mean}(Gy)$	30.32	29.43
R-Parotid	$V_{30Gy}(\%)$	33.78	32.67
	$V_{50Gy}(\%)$	13.99	12.47
	$D_{mean}(Gy)$	26.62	25.92

reasons: First, no matter whether the calculated gEUD in the given optimized plan was greater or less than the prescribed gEUD0, the improved gEUD regularized sub-score in (6) contributed to the optimization. Therefore, the solution space is enlarged. Second, the improved gEUD-based hybrid criteria optimization model in (7) has continuous and non-zero gradients in all the feasible solution space, which can not be guaranteed in original gEUD-based optimization model containing linear gEUD sub-score. Third, the original linear gEUD-based sub-score was not increasing function, and thus could not guarantee that optimized plans based on them would be Pareto optimal [3]. Our proposed gEUD-based regularized sub-score, however, is an increasing function that can guarantee Pareto optimality. All these reasons discussed above show that the improved gEUD-based hybrid criteria optimization model has the ability to fruitfully expand the search space.

In theory, the organ evaluation criteria (OEC) Pareto surface(i.e., XOEC) belongs to the DVH Pareto surface (i.e., XDVH) [3], the plan optimized based on the organ evaluation model can be obtained by dose volume optimization based on the dose-volume (DV) constraints. As shown in Fig.8, for prostate cancer case, the DVH plan generated by using two DV constraints for PTV, three DV constraints for Bladder, and for DV constraints for Rectum, was comparable to the improved plan as far as OARs protection and PTV coverage. That is to say that the quality of DV plan is similar to that of the improved plan. the finding was also verified for all testing cases. However more sub-scores were needed in DV optimization model. Increase in the number of sub-scores increases the complexity of parameters adjustment, and hence is time consuming. So our proposed optimization model has potential to improve the efficiency of treatment planning.

Through the investigation of the influence of regularization parameter ε on the plan quality, we can conclude that with the increase of regularization parameters, the improved plan quality is better than the unimproved plan. However, when the regularization parameters ε is increased to a certain level, such as 0.5, the differences between the both plans will no longer be obvious.
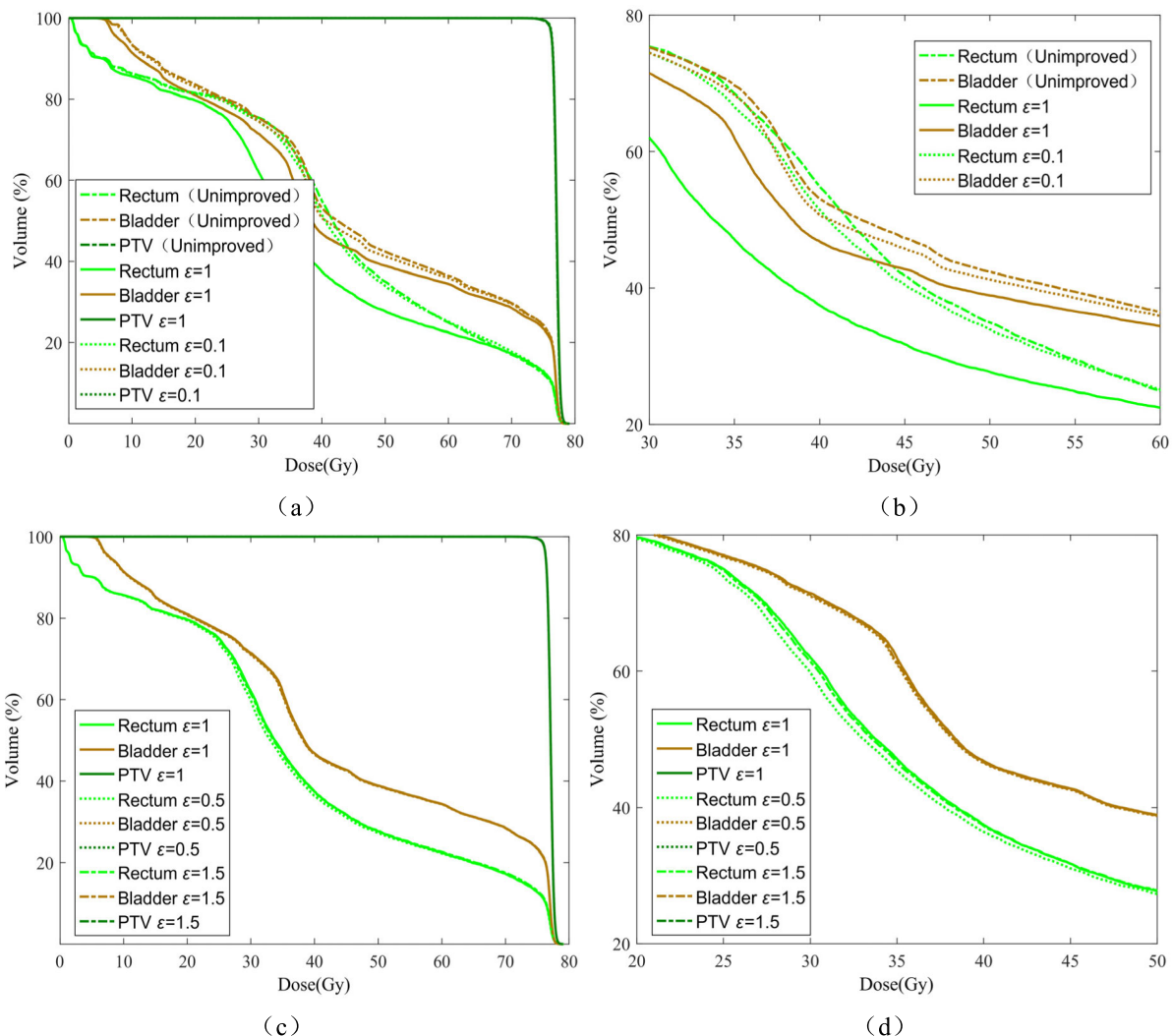
FIGURE 7. Influence of regularization parameters ε on optimization results. (a) DVH comparisons between improved plan ($\varepsilon = 1$ and $\varepsilon = 0.5$) and the unimproved plan; (b) the detail part of the Fig.(a); (c) DVH comparisons of improved plan($\varepsilon = 1$, $\varepsilon = 0.5$ and $\varepsilon = 1.5$).
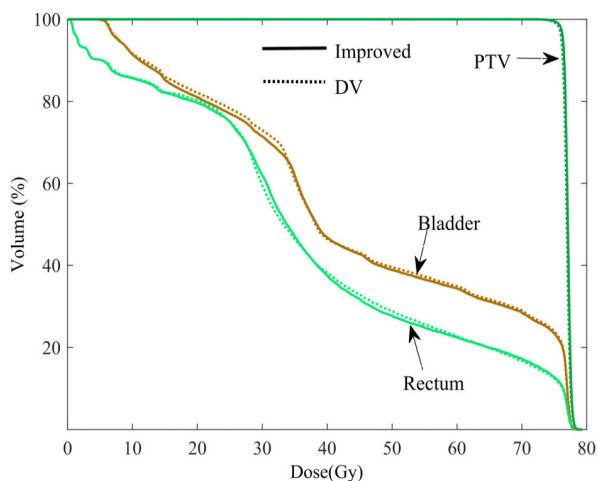

FIGURE 8. DVH comparisons between the improved plan and the DV plan on prostate cancer case.

In our previous work [2], a new piecewise penalty gEUD sub-score was proposed to overcome the semi-deviation and

gradient vanishing of the linear gEUD sub-score. However, the problem of the gradient discontinuous at the cut-off point is also existing. In the improved regularized gEUD sub-score, the problems of semi-deviation, gradient vanishing, and gradient discontinuous were all solved. Testing on prostate cancer case, the DVH comparisons between the unimproved plan, improved plan regularized gEUD sub-score (denoted by *lse*) and the piecewise plan using piecewise penalty gEUD sub-score (denoted by *piecewise*) was shown in Fig.9. The *lse* plan and the piecewise plan were very similar, and they were clearly better than the unimproved plan. The regularization parameters ε contained in the *lse* gEUD sub-score can increase the flexibility of the optimization model to control the plan quality.

V. CONCLUSION
To improve the quality of radiotherapy plan, the main purpose of this paper was to construct a new gEUD-based hybrid criteria optimization model to preliminarily solve the problems of semi-deviation, the vanishing gradient and non-increasing
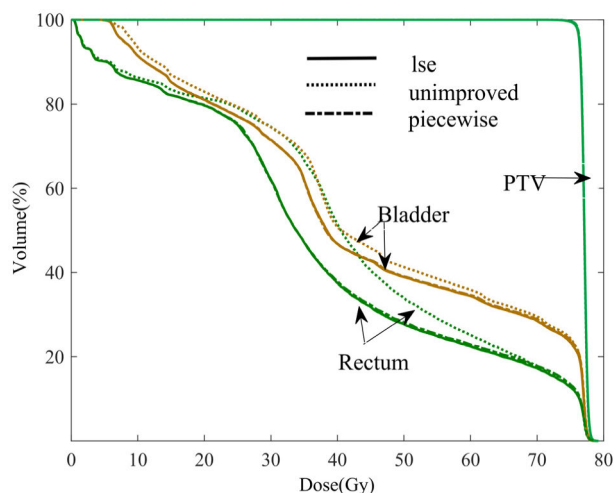
FIGURE 9. DVH comparisons among unimproved plan, lse plan and piecewise plan for prostate case.

in the feasible solution space, prevalent in the optimization model. The new gEUD-based hybrid criteria optimization model was proposed based on regularization theory.

From the results of this research and our previous work, it can be concluded that the structure of optimization model has an important influence on the search ability of optimization algorithms, especially for gradient-based optimization algorithms. Optimization models, which are increasing, continuous and non-zero gradient in all the solution space, have the ability to expand the search solution space. When these optimization models are used in radiotherapy planning, better radiotherapy plans can be gained. This improvement is significant. In most radiotherapy planning, once the optimized plan satisfies predefined requirements, the planning stops, not only because of limited radiation resources, but also because of uncertainty concerning the optimal plan. Our proposed method can improve the quality of acceptable plans by using a modified optimization model, which should be helpful in further strengthening PTV coverage and increasing the gain ratio of radiotherapy.

There persist challenges and room for improvement in this vein. First, the manner in which we adjust the regularization parameter ε, remains heuristic, due to the uncertain relationship between DVH curves and it. We need to investigate an efficient way to determine ε. Second, we only applied the new gEUD-based optimization model in the fluence map optimization (FMO) omitting the segmentation of beamlet intensity. In future study, we need to include the new optimization model into the segmentation of beamlet intensity. Third, weighting factors are important parameters in the optimization model. In our study, they were adjusted by trial and error. In future study, we need to include the automatic weighting factors optimization into the radiotherapy planning. At last, the new optimization model should be applied in some more clinical cases to test its efficiency.

Finally, the proposed new optimization model can not only be used in IMRT inverse treatment planning, but can also other radiation field, such as direct aperture optimization (DAO), volumetric modulated arc therapy plans, etc., While the prostate and HN are partial tumor sites, there is potential for applying the novel gEUD-based optimization model to other tumor sites. Related work is in progress. In addition, the influences of the optimization models on the other optimization algorithms, such as heuristic optimization algorithms, should be paid more attention in future work.

REFERENCES

[1] G. Kalantzis and A. Apte, "A novel reduced-order prioritized optimization method for radiation therapy treatment planning," *IEEE Trans. Biomed. Eng.*, vol. 61, no. 4, pp. 1062–1070, Apr. 2014.

[2] C. Guo, P. Zhang, L. Zhang, Z. Gui, and H. Shu, "Application of optimization model with piecewise penalty to intensity-modulated radiation therapy," *Future Gener. Comput. Syst.*, vol. 81, pp. 280–290, Apr. 2018.

[3] M. Zarepisheh, A. F. Uribe-Sanchez, N. Li, X. Jia, and S. B. Jiang, "A multicriteria framework with voxel-dependent parameters for radiotherapy treatment plan optimization," *Med. Phys.*, vol. 41, no. 4, Apr. 2014, Art. no. 041705.

[4] L. Zhang, Z. Gui, J. Yang, and P. Zhang, "A column generation approach based on region growth," *IEEE Access*, vol. 7, pp. 31123–31139, 2019.

[5] L. Zhang, P. Zhang, J. Yang, J. Li, and Z. Gui, "Aperture shape generation based on gradient descent with momentum," *IEEE Access*, vol. 7, pp. 157623–157632, 2019.

[6] P. Zhang, L. Zhang, J. Yang, and Z. Gui, "The aperture shape optimization based on fuzzy enhancement," *IEEE Access*, vol. 6, pp. 35979–35987, 2018.

[7] Y. Mai, F. Kong, Y. Yang, L. Zhou, Y. Li, and T. Song, "Voxel-based automatic multi-criteria optimization for intensity modulated radiation therapy," *Radiat. Oncol.*, vol. 13, no. 1, p. 241, Dec. 2018.

[8] A. L. Hoffmann, D. D. Hertog, A. Y. D. Siem, J. H. A. M. Kaanders, and H. Huizenga, "Convex reformulation of biologically-based multi-criteria intensity-modulated radiation therapy optimization including fractionation effects," *Phys. Med. Biol.*, vol. 53, no. 22, pp. 6345–6362, Oct. 2008.

[9] Q. Diot, B. Kavanagh, R. Timmerman, and M. Miften, "Biological-based optimization and volumetric modulated arc therapy delivery for stereotactic body radiation therapy," *Med. Phys.*, vol. 39, no. 1, pp. 237–245, Jan. 2012.

[10] J. Yang, P. Zhang, L. Zhang, H. Shu, B. Li, and Z. Gui, "Particle swarm optimizer for weighting factor selection in intensity-modulated radiation therapy optimization algorithms," *Phys. Med.*, vol. 33, pp. 136–145, Jan. 2017.

[11] C. Guo, P. Zhang, Z. Gui, H. Shu, L. Zhai, and J. Xu, "Prescription value-based automatic optimization of importance factors in inverse planning," *Technol. Cancer. Res. Treat.*, vol. 18, pp. 1–13, Apr. 2019.

[12] *Biological Optimization Using the Equivalent Uniform Dose (EUD) in Pinnacle*[3], RaySearch Lab., Stockholm, Sweden, Feb. 2003.

[13] M. Hartmann and L. Bogner, "Investigation of intensity-modulated radiotherapy optimization with gEUD-based objectives by means of simulated annealing," *Med. Phys.*, vol. 35, no. 5, pp. 2041–2049, Apr. 2008.

[14] T. Dirscherl, J. Alvarez-Moret, and L. Bogner, "Advantage of biological over physical optimization in prostate cancer?" *Zeitschrift Med. Phys.*, vol. 21, pp. 228–235, Sep. 2011.

[15] L. Widesott, L. Strigari, M. C. Pressello, M. Benassi, and V. Landoni, "Role of the parameters involved in the plan optimization based on the generalized equivalent uniform dose and radiobiological implications," *Phys. Med. Biol.*, vol. 53, no. 6, pp. 1665–1675, Feb. 2008.

[16] M. Schwarz, J. V. Lebesque, B. J. Mijnheer, and E. M. F. Damen, "Sensitivity of treatment plan optimisation for prostate cancer using the equivalent uniform dose (EUD) with respect to the rectal wall volume parameter," *Radiotherapy Oncol.*, vol. 73, pp. 209–221, Nov. 2004.

[17] Q. Wu, D. Djajaputra, Y. Wu, J. Zhou, H. H. Liu, and R. Mohan, "Intensity-modulated radiotherapy optimization with gEUD-guided dose–volume objectives," *Phys. Med. Biol.*, vol. 48, no. 3, pp. 279–291, Mar. 2015.

[18] D. N. Mihailidis, B. Plants, L. Farinash, M. Harmon, L. Whaley, P. Raja, and P. Tomara, "Superiority of equivalent uniform dose (EUD)-based optimization for breast and chest wall," *Med. Dosimetry*, vol. 35, no. 1, pp. 67–76, Mar. 2010.

[19] T. F. Lee, H.-M. Ting, P.-J. Chao, H.-Y. Wang, C.-S. Shieh, M.-F. Horng, J.-M. Wu, S.-A. Yeh, M.-Y. Cho, E.-Y. Huang, Y.-J. Huang, H.-C. Chen, and F.-M. Fang, "Dosimetric advantages of generalised equivalent uniform dose-based optimisation on dose–volume objectives in intensity-modulated radiotherapy planning for bilateral breast cancer," *Brit. J. Radiol.*, vol. 85, pp. 1499–1506, Nov. 2012.

[20] A. Fredriksson, "Automated improvement of radiation therapy treatment plans by optimization under reference dose constraints," *Phys. Med. Biol.*, vol. 57, no. 23, pp. 7799–7811, Nov. 2012.

[21] T. Zhang, R. Bokrantz, and J. Olsson, "Direct optimization of dose–volume histogram metrics in radiation therapy treatment planning," *Biomed. Phys. Eng. Exp.*, vol. 6, no. 6, Oct. 2020, Art. no. 065018.

[22] W. Huyer and A. Neumaier, "A new exact penalty function," *SIAM J. Optim.*, vol. 13, no. 4, pp. 1141–1158, Jan. 2003.

[23] A. Niemierko, "A generalized concept of equivalent uniform dose (EUD)," *Med. Phys.*, vol. 26, no. 6, p. 11110, Jan. 1999.

[24] B. Choi and J. O. Deasy, "The generalized equivalent uniform dose function as a basis for intensity-modulated treatment planning," *Phys. Med. Biol.*, vol. 47, no. 20, pp. 3579–3589, Oct. 2002.

[25] D. Craft, M. Bangert, T. Long, D. Papp, and J. Unkelbach, "Shared data for intensity modulated radiation therapy (IMRT) optimization research: The CORT dataset," *GigaScience*, vol. 3, no. 1, p. 37, Dec. 2014.

[26] E. Dale, T. P. Hellebust, A. Skjønsberg, T. Høgberg, and D. R. Olsen, "Modeling normal tissue complication probability from repetitive computed tomography scans during fractionated high-dose-rate brachytherapy and external beam radiotherapy of the uterine cervix," *Int. J. Radiat. Oncol. Biol. Phys.*, vol. 47, no. 4, pp. 963–997, Jul. 2000.

[27] S. T. Peeters, M. S. Hoogeman, W. D. Heemsbergen, A. A. M. Hart, P. C. M. Koper, and J. V. Lebesque, "Rectal bleeding, fecal incontinence, and high stool frequency after conformal radiotherapy for prostate cancer: Normal tissue complication probability modeling," *Int. J. Radiat. Oncol. Biol. Phys.*, vol. 66, no. 1, pp. 11–19, Sep. 2006.

[28] E. B. Butler, B. S. Teh, W. H. Grant, B. M. Uhl, R. B. Kuppersmith, J. K. Chiu, D. T. Donovan, and S. Y. Woo, "Smart (simultaneous modulated accelerated radiation therapy) boost: A new accelerated fractionation schedule for the treatment of head and neck cancer with intensity modulated radiotherapy," *Int. J. Radiat. Oncol. Biol. Phys.*, vol. 45, no. 1, pp. 21–32, Aug. 1999.

[29] J. O. Deasy, A. I. Blanco, and V. H. Clark, "CERR: A computational environment for radiotherapy research," *Med. Phys.*, vol. 30, no. 5, pp. 979–985, May 2003.

[30] L. B. Marks, E. D. Yorke, A. Jackson, R. K. T. Haken, L. S. Constine, A. Eisbruch, S. M. Bentzen, J. Nam, and J. O. Deasy, "Use of normal tissue complication probability models in the clinic," *Int. J. Radiat. Oncol. Biol. Phys.*, vol. 76, no. 3, pp. S10–S19, Mar. 2010.

[31] X. C. Zhang, M. Shi, F. Xiao, C. Y. Sun, Y. Zhu, X. L. Liu, and J. Wang, "Impact of radiation dose-volume on parotid salivary recovery in nasopharyngeal cacinomapatients with intensity-modulated radiotherapy," *Chin. J. Cancer Prevention Treat.*, vol. 16, no. 6, pp. 447–450, Mar. 2009.

CAIPING GUO received the Ph.D. degree in signal and information processing from the North University of China, Shanxi, China, in 2018.

She is currently an Associate Professor with the College of Taiyuan Institute of Technology. Her research interests include in the area of signal processing and radiotherapy optimization.

• • •